

Early fault diagnostic system for rolling bearing faults in wind turbines

Libowen Xu,

Department of Engineering, Durham University
South Road, Durham, DH1 3LE U.K.
libowen.xu@durham.ac.uk

Qing Wang¹

Department of Engineering, Durham University
South Road, Durham, DH1 3LE U.K.
qing.wang@durham.ac.uk

Ioannis Ivrissimtzis

Department of Computer Science, Durham University
South Road, Durham, DH1 3LE U.K.
ioannis.ivrissimtzis@durham.ac.uk

Shisong Li

Department of Engineering, Durham University
South Road, Durham, DH1 3LE U.K.
shisong.li@durham.ac.uk

ABSTRACT

The operation and maintenance costs of windfarms are always high due to high labour costs and the high replacement cost of parts. Thus, it is of great importance to have real-time monitoring and an early fault diagnostic system to prevent major events, reduce time-based maintenance and minimize the cost. In this paper, such a 2-step system for early stage rolling bearing failures in off-shore wind turbines is introduced. Firstly, Empirical Mode Decomposition (EMD) is applied to minimize the effect of ambient noise. Next, correlation coefficients between a reference signal and test signals are obtained and incipient fault detection is achieved by comparing the results with a threshold value. Through further analysis of the envelope

¹ Corresponding author

spectrum, Sample Entropy for selected Intrinsic Mode Functions is obtained, which is further used to train a Support Vector Machine classifier to achieve fault classification and degradation state recognition. The proposed diagnostic approach is verified by experimental tests, and an accuracy of 98% in identifying and classifying rolling bearing failures under various loading conditions is obtained.

1 INTRODUCTION

With ever-increasing energy demands, renewable energies such as wind power are becoming increasingly attractive for both financial investors and governments around the world. The fast development in wind industry has also accelerated the operation and maintenance business (O&M) due to the need to maintain power generation efficiency. In fact, the global O&M market is forecasted to reach \$20.6 billion by 2023 [1]. However, some argue that with the usual method of sending a maintenance team after the failure, the downtime for offshore wind turbines can be up to 13 days, resulting in increased losses [2]. Thus, the design of a complete and accurate diagnostic system is deemed necessary, even critical for both wind farm developers and O&M business investors.

Among all the components, high-speed rolling bearings are those of the greatest importance to wind turbines owing to their support to both axial and tangential loads. Faults in bearings can lead to a catastrophic failure of the entire system, and hence the maintenance is essential. In order to establish such a system, three major steps need to be addressed: 1) accurate real-time monitoring, 2) early fault detection, and 3) classification of existing defects and degradation states.

Firstly, an effective real-time monitoring method needs to be applied to obtain continuous vibration data from the machine before applying various signal processing

methods. Among all monitoring techniques, the most common solution is to install accelerometers on rotating machines and obtain the vibration signal in the time domain.

In real working conditions, there exists a large amount and variety of inevitable noise, which often embodies strong vibrations from several competing sources and spans across a large frequency range, e.g., random impacts from friction and contact forces or external disturbances [3]. In the early stage of defect development, the defect vibration signal is weak and can be easily masked by noise. Thus, it is essential to find a way of extracting high quality features from the early-stage failure.

Up to now, a range of feature extraction approaches have been developed, which can be broadly classified into four categories [4]: 1) time-domain feature extraction, 2) frequency-domain feature extraction, 3) time-frequency representation, and 4) complexity measurement.

Time-domain analysis is considered as the most classic approach to distinguish between different vibration signals. Time domain features, including statistical features (RMS, variance, skewness, and kurtosis) and non-dimensional features (shape factor, crest factor, impulse factor, and margin factor) have been widely used in past research [5]. Additionally, mathematical morphology operators, which were formerly introduced as a non-linear method to analyse two-dimensional image data [6], had been proved to be effective in detecting rolling bearing defect frequencies in wind turbines[7,8].

To perform frequency-domain analysis, the time-domain vibration signal needs to be transformed into a frequency-domain signal, and the most common and

representative way is to apply the Fourier transform, usually implemented in the form of Fast Fourier Transform (FFT) [9]. In this way, frequency domain features including spectral skewness and spectral kurtosis can be extracted and used to identify rolling bearing failures [10,11]. In the existing literature, researchers have already modified the method for specified high-speed wind turbine bearing failures [12].

Time-frequency representation methods aim at finding the frequency components of the signal, as well as how the instantaneous frequency and amplitude of a certain component varies within a certain time window. Within the field of time-frequency representation, wavelet transform and Empirical Mode Decomposition based time-frequency analysis are the two most representative methods.

Wavelet transform is a well-known method in analysing non-stationary signals and has been developed over several decades [13,14,15]. By choosing the appropriate wavelet basis, the wavelet transform methods can approximate well the signal with a limited number of coefficients [16]. Through this process, the selected coefficients can be used as defect features for rolling bearings inside wind turbines [17, 18].

Adaptive signal processing is another direction of research in the area of time-frequency representation. In the current literature, the most representative method is Empirical Mode Decomposition [19]. This method is based on sequential extraction of energy associated with various intrinsic time scales of the signal, starting from high frequency modes to low frequency modes [19]. Through the decomposition process, sensitive signal components can be selected and used for further feature extraction.

Complexity measurements such as approximate entropy and sample entropy are used for assessing the complexity of time domain signals. Approximate entropy (ApEn), developed by Steve M. Pincus, is a technique used to quantify the regularity and unpredictability of time series fluctuations [20]. The larger the value of ApEn, the more the unpredictability of the behaviour of the signal. Sample entropy (SampEn) is a modification of approximate entropy and the process of its computation does not depend on the size of the dataset [21]. To date, both ApEn [22] and SampEn [23] have been studied and directly used by researchers in the field of extraction of wind bearing fault features.

Other feature extraction methods including correlation dimension [24], Singular Value Decomposition (SVD) [25], piecewise Aggregate Approximation (PAA) [26] and Kolmogorov-Smirnov (KS) Test [27] were also applied to identify rolling bearing failures, obtaining promising results in multiple cases and could be further optimized for wind turbine bearing problems.

After retrieving defect features, a tool is needed to automatically recognise faults in order to realize automatic diagnosis. Over the past two decades, the use of machine learning techniques have developed from a mere speculative idea into a broad topic of research. Due to their high accuracy fault classification, they are also favoured by researchers focusing in this particular area: Sugumaran used a decision tree for fault diagnostics of roller bearings [28]; Pandya used multinomial logistic regression techniques [29]; and Lin et al applied a support vector machine based on an artificial fish-swarm algorithm [30]. Apart from these traditional machines learning approaches, deep learning

models including CNNs (convolutional neural network) and RNNs (recurrent neural networks) [31,32] have been adapted into the design of a rolling bearing prognostic system. Furthermore, some researchers have modified LSTMs (Long short-term memory) [33] using data from wind turbine shafts to achieve early fault diagnosis. However, the deep learning models proved to have better performance only with a large sample pool, which makes them less suitable in this case, where there is a limited number of training data available.

Among the machine learning methods, a Support Vector Machine (SVM) is a general learning method, well-grounded on Statistical Learning Theory [34], which particularly effective in cases with small sample pool. Also, it has a relatively simple structure and a satisfying generalization ability, which makes it particularly suitable for solving real life failure diagnosis problems.

In this paper, a high-speed rolling bearing status diagnosis system for wind turbines based on high-quality feature extraction and Support Vector Machine is proposed. The idea is to merge the merits of several individual techniques into one whole diagnostic system. Through case studies, the proposed system exhibits a high accuracy for rolling bearing faults detection and classification (over 98%) across various loading conditions in a noisy environment. The proposal also offers a way for bearing degradation status recognition, and it shows improved performance (75% accuracy) over ordinary time-domain and frequency-domain feature extraction methods.

The remainder of this paper is organized as follows: Section 2 presents the overall framework of the prognostic system and introduces the methods used in this paper; In Section 3, the system proposed in this paper is validated through experiments using data collected from bearing run-to-failure tests. The results are also critically compared with other deep-learning models and feature extraction methods. Section 4 draws some conclusions based on the performance of the system and suggests the further work that can be done.

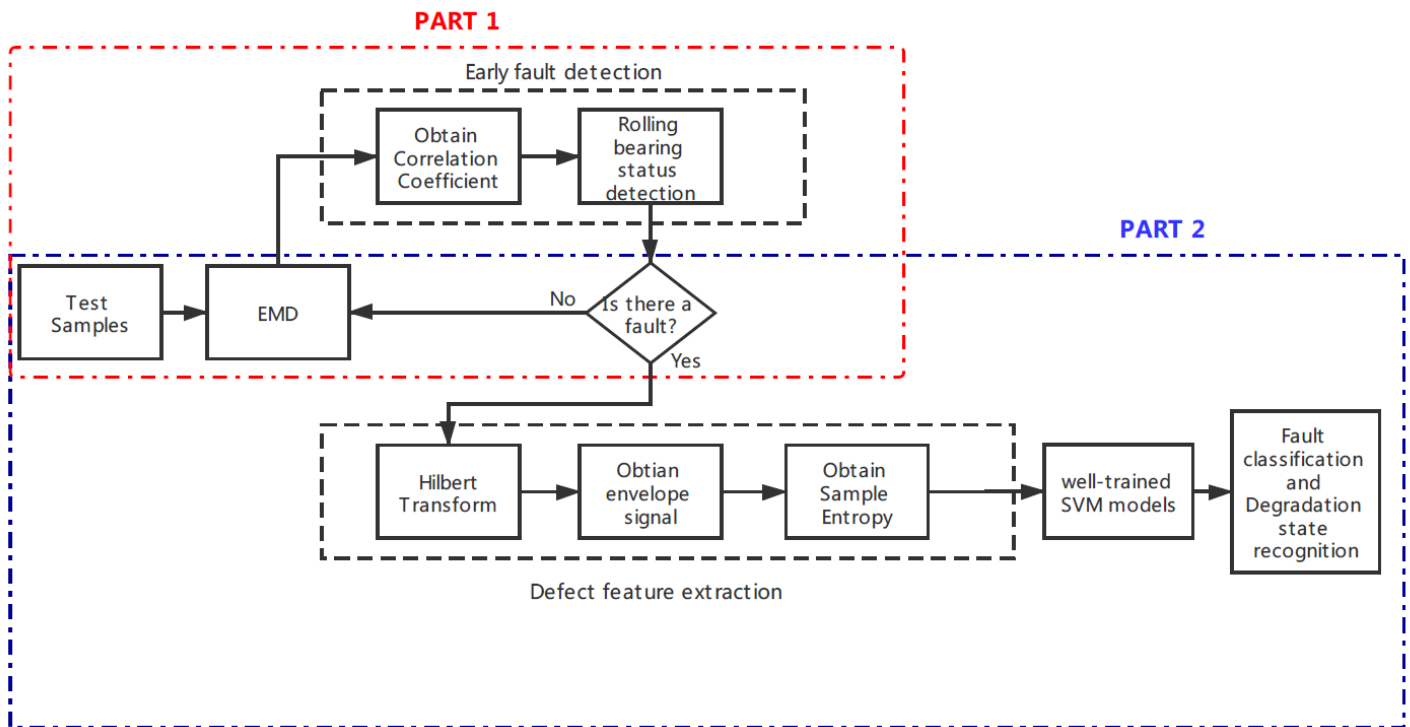
2 DIAGNOSTIC PRINCIPLES

2.1 ROLLING BEARING DIAGNOSTIC SYSTEM

Figure 1 illustrates the structure of the proposed high-speed rolling bearing diagnostic system. The system uses the vibration signal retrieved as input. Firstly, EMD is applied to the input signal. This step is a data pre-processing step with two main purposes: 1) it denoises the signal and 2) IMFs that contain bearing failure information can be selected out. Next, correlation coefficients are obtained between the signal and reference signal and compared with a threshold value to identify where the bearing is under fault state. If the bearing is under a certain fault state, a Hilbert Transform will be applied to the selected IMFs to obtain the envelope signal. During this process, the signal is demodulated and the energy concentrated at the defect frequency is highlighted. As a result, the processed signal is ready for feature extraction. To extract features that have the lowest dimension possible and can best represent one specific fault status, Sample Entropy is obtained for every envelope signal and further grouped up as a feature matrix.

Finally, through two well-trained SVM classifiers, both the rolling bearing fault and degradation state can be identified.

The core idea of the proposal is the selection of different data analysis techniques and their adaptive arrangement for rolling bearing diagnostics. To lay a theoretical foundation, these major techniques, i.e. the Hilbert Huang Transform, the Pearson



correlation coefficient calculation, the sample entropy, as well as the Support Vector Machines, are briefly discussed in the next subsections.

Fig.1 Flow chart for rolling bearing diagnostic system

2.2 Empirical Mode Decomposition based time-frequency analysis

In 1999, Huang, with his team, proposed the Empirical Mode Decomposition (EMD), which is an adaptive signal decomposition method based on sequential extraction of energy associated with various intrinsic time scales of the signal, starting from high

frequency modes and going to low frequency modes [19]. For a data series $x(t)$, EMD is implemented through a sifting process which follows the rules below [19]:

1) Identify all the local extrema and connect all local maxima (minima) on $x(t)$ with a cubic spline as the upper (lower) envelope.

2) Calculate local mean $m_1(t)$ for the two envelopes and further obtain $d_1(t) = x(t) - m_1(t)$.

3) Unless the two criteria mentioned above are satisfied, treat $d_1(t)$ as the data and repeat steps 1 and 2 until the envelopes are symmetric with respect to the zero mean. The final $d_k(t)$ is designated as $c_n(t)$.

4) The sifting process stops when the residue r_n becomes a monotonic function or a function with only one extremum from which no more intrinsic mode function (IMF) can be extracted.

The process can be described as:

$$x(t) = \sum_{i=1}^n c_i + r_n \quad (1)$$

Through the decomposition process, n IMFs were created. However, not all the IMFs can be used to analyse and determine the nature of the waveform. This is because during the decomposition procedure, the energy will often be concentrated on the high frequency modes (first IMFs) and then it keeps decreasing until the last IMF is created. According to this idea, the last IMFs represents the noise signal, given that the energy distribution of the useful components (signal) is not big enough to overcome that of the noise signal.

To further analyse the mode functions, a Hilbert Transform was applied. With an existing signal $x(t)$, its Hilbert Transform $H[x(t)]$ takes the form:

$$H[x(t)] = \frac{1}{\pi} \sum_{-\infty}^{+\infty} \frac{x(\tau)}{t - \tau} d\tau \quad (2)$$

where $H[x(t)]$ is the convolution of $x(t)$ and $\frac{1}{\pi t}$.

The Hilbert transform is important in signal processing as it can derive the analytic representation of a real-valued signal, which can be further utilized to calculate the instantaneous frequency and amplitude of the signal [19].

2.3 Pearson Correlation Coefficient

The Pearson correlation coefficient (PCC) is a parameter that measures linear correlation between two variables X and Y . It has a value between +1 and -1. A value of +1 is total positive linear correlation, 0 is no linear correlation, and -1 is total negative linear correlation. By computing PCC, one can easily know if there is linear correlation between two sets of data. For given signals $x(n)$ and $y(n)$, the Pearson correlation coefficient ρ is the covariance of the variables divided by the product of their standard deviations [35]. The formula for the Pearson correlation coefficient can be written as:

$$\rho_{X,Y} = \frac{cov(X, Y)}{\sigma_X \sigma_Y} \quad (3)$$

Since the product of $\sigma_X \sigma_Y$ is a constant, the value of $\rho_{X,Y}$ is determined by the covariance of signal X, Y :

$$\text{cov}(X, Y) = \exp[(X - \mu_X)(Y - \mu_Y)] \quad (4)$$

where: μ_X is the mean of X and μ_Y is the mean of Y .

2.4 Sample Entropy

Richman and Moorman [21] proposed the idea of Sample Entropy, a technique used to quantify the amount of regularity and unpredictability of fluctuations over time-series data: the greater the probability of generating a new pattern in the series, the greater the complexity of the sequence which thus leads to greater entropy. This is because the complexity and unpredictability of the rolling bearing vibration signal will increase as the defect grows. Thus, it is a logical choice to use Sample Entropy as an indicator in fault diagnosis.

For a time-series dataset: $\{X(n)\}, n = 1, 2, \dots, n$, Sample Entropy is calculated through the following process:

1) Define a template vector of dimension m : $X_m(i), i = 1, 2, \dots, N - m + 1$, where $X_m(i) = \{x(i), x(i + 1), \dots, x(i + m - 1)\}$.

2) Define the distance function $d[X_m(i), X_m(j)]$ ($i \neq j$) ($j \in [1, N - m + 1]$) to be the Chebyshev distance, that is:

$$d[X_m(i), X_m(j)] = \max_{k=0, \dots, m-1} (|x(i + k) - x(j + k)|) \quad (5)$$

3) Define tolerance r . For $1 \leq i \leq N - m + 1$, let B_i be the number of $X_m(j)$ such that $d[X_m(i), X_m(j)] \leq r$ and define $B_i^m(r)$ as the probability that any vector $X_m(j)$ is within r of $X_m(i)$:

$$B_i^m(r) = (N - m + 1)^{-1} * B_i \quad (6)$$

4) Let $k = m+1$ and repeat step 1-3, define $A_i^k(r)$:

$$A_i^k(r) = (N - k)^{-1} * A_i \quad (7)$$

5) Calculate the average of natural logarithms of the functions $B_i^m(r)$ and $A_i^k(r)$ for every i and denote the results as B^m and A^k :

$$B^m(r) = (N - m + 1)^{-1} * \sum_{i=1}^{N-m+1} B_i \quad (8)$$

$$A^k(r) = (N - m + 1)^{-1} * \sum_{i=1}^{N-k} A_i \quad (9)$$

(6) Define the sample entropy:

$$SampEn(m, r, N) = -\ln \frac{A^k(r)}{B^m(r)} \quad (10)$$

According to Richman and Moorman's research [21] and through the process of trial and error, the values of m and r were usually chosen between 1 and 2, and 0.15SD to 0.2SD, respectively (SD denotes standard deviation).

2.5 Support Vector Machines

Support Vector Machines is a classical high dimensional, non-linear classification that specializes in dealing with cases of a small sample pool. Its main idea is to find an optimal hyperplane to maximise the margin between different classes. In two-dimensional space, the hyperplane is a line dividing a plane into two parts where each

class lies on either side (Figure 2(a)). A detailed description of this method can be found in [34].

In this paper, defect features cannot be linearly separated. In this case, support vector machine uses the kernel function to map the original sample data into a higher dimensional space, and the decision function will be:

$$f(x) = \text{sgn} \left(\sum_{i,j=1}^M \alpha_i y_i K(x_i^T x_j) + b \right) \quad (11)$$

Additionally, the kernel function used in this paper is the Radial Basis Function (RBF), which is defined as:

$$K(x_i, x_j) = \exp \left(-\gamma \|x_i - x_j\|^2 \right) \quad (12)$$

Where the value of γ in this paper is obtained using a cross-validation method (partitioning the data into subsets, training the data on a subset and using the other subset to evaluate the model's performance).

In all, an SVM is a binary classification model. To adapt and optimize the performance of SVM on a multi-class classification problem, a one-vs-one SVM strategy (Figure 2(b)) is used in this paper: for a multi-class case with k classes, $k(k-1)/2$ SVM models need to be trained, with each SVM models corresponding to one binary classification problem. Finally, through a cross-validation process, optimal training parameters are selected.

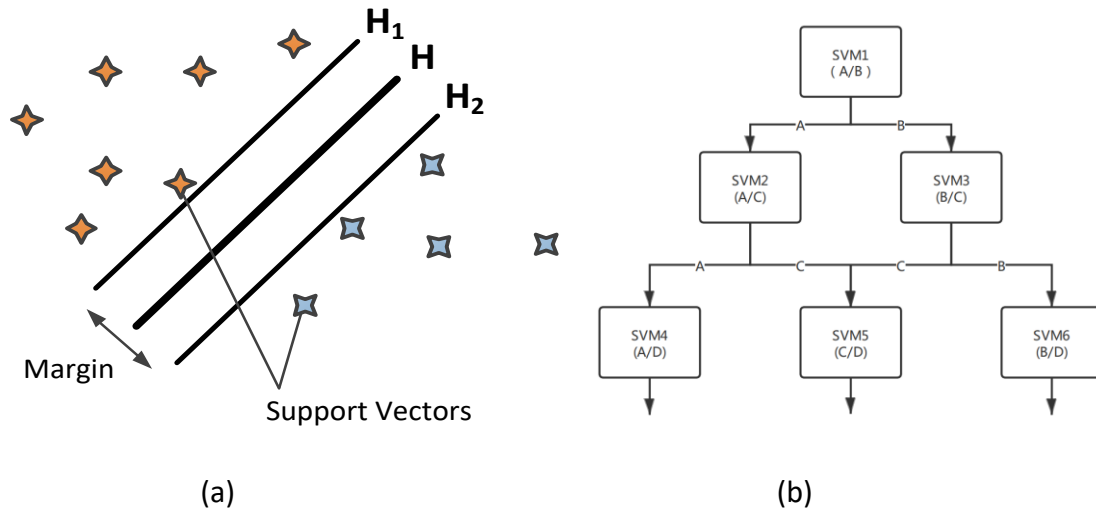


Fig.2 (a): Support vector optimal classification plane. (b): The illustration of one-vs-one SVM strategy.

3 CASE STUDIES

The first and third parts in this section use experimental data from IMS (Intelligent Maintenance System) test to failure experiments from the University of Cincinnati [36]. The second part uses experimental data from the bearing data centre of Case Western Reserve University [37].

3.1 Early Fault Detection based on EMD and Pearson Correlation Coefficient

From nearly five decades of study into the rolling bearing failure mechanism, researchers found that defects tend to follow similar patterns, although they may possess different features. The defect starts with two components of a rolling bearing in contact; thus, a defect meets its mating surface, generating a characteristic impulse. The frequency of occurrence of the impulse is referred to as the characteristic defect frequency. The frequency is very high and can sometimes reach 20kHz. Thus, the high-frequency part of the signal is very sensitive to the change in bearing working conditions.

By using this feature and knowing that the first IMF created by EMD will always contain the high frequency component of the original signal, it is obvious that when a defect exists, the correlation coefficient obtained between the test and vibration signals under normal working conditions will vary greatly compared to the correlation coefficient corresponding to a 'healthy' test signal.

The test rig has four test bearings on one shaft. The shaft is driven by an AC motor and coupled by rub belts. Detailed bearing dimensions are shown in Table 1.

Table 1. Detailed bearing dimensions of test rig 1

Pitch diameter/mm	Roller diameter/mm	Contact Angle/degree	No. rollers
71.5	8.41	15.17	16

The experiment lasts for 164 hours with a sampling interval of 10 minutes. The data is collected with a sampling rate of 20kHz by a National Instruments DAQCard-6062E data acquisition card. At the end of the experiment, outer race failure occurred in bearing 1. Without knowing the nature of the bearing test-to-failure data, we first assume data acquired in the first 12 hours are considered to be 'healthy signals', which are the vibration signals recorded under normal working condition. Among these 'healthy signals', one reference signal is randomly chosen to be the baseline signal. EMD is applied to this signal and the first IMF is chosen, followed by Fourier Transform applied to this IMF to obtain the frequency spectrum. The same procedure is conducted on the other 50 randomly chosen 'healthy signals' and their correlation coefficients with the reference signal are computed and plotted in Figure 3(a). From the plot, it is clear that the 50

coefficients obtained fluctuate slightly within the range of 0.47-0.54. Figure 4 gives the illustration of the reference signal from both time-domain and frequency-domain aspects.

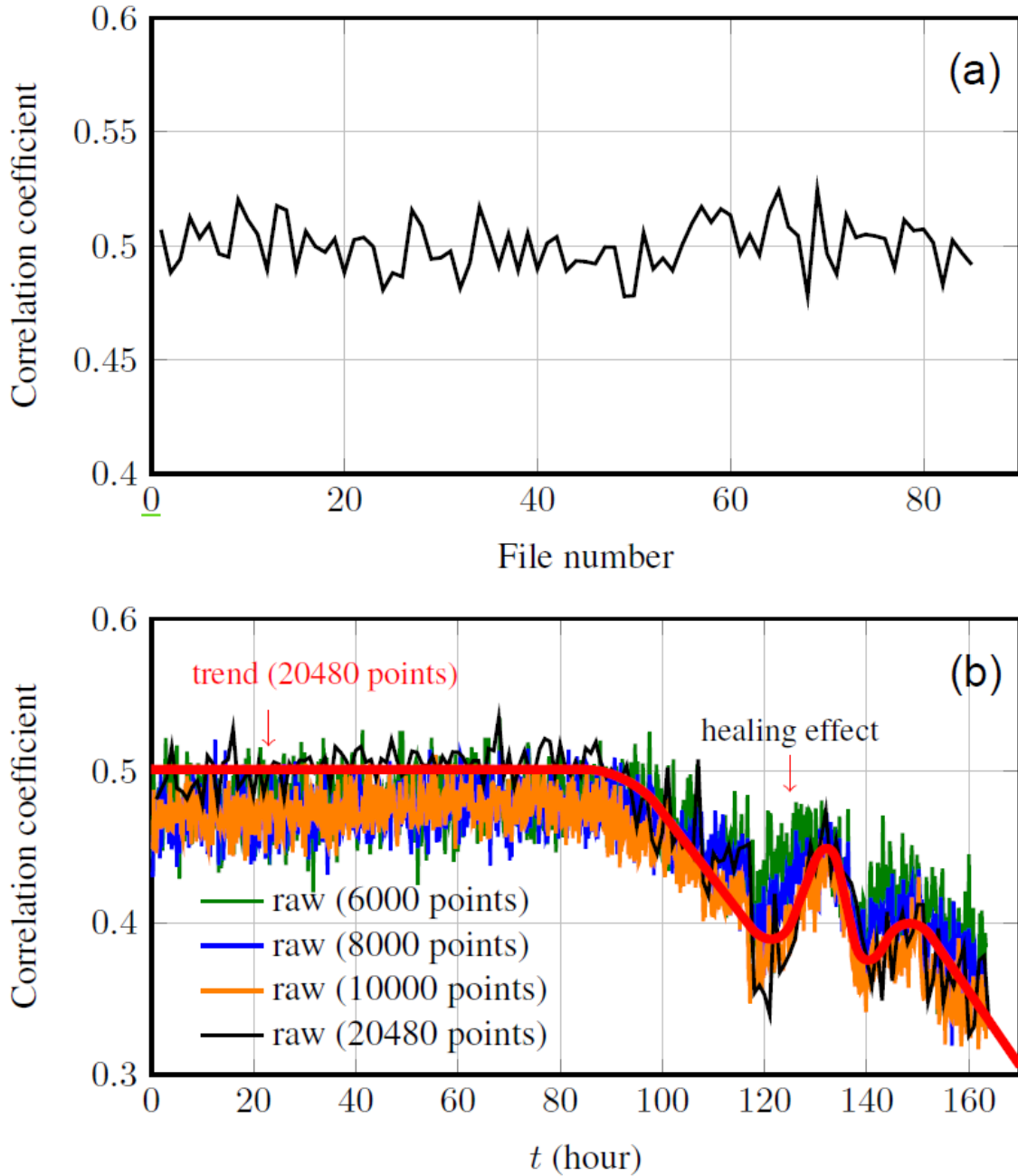


Fig.3 (a): Illustration of the reference signal and the correlation coefficients obtained between the reference signal and other 'healthy signal'. (b): illustrations of the change in correlation coefficient with bearing working time.

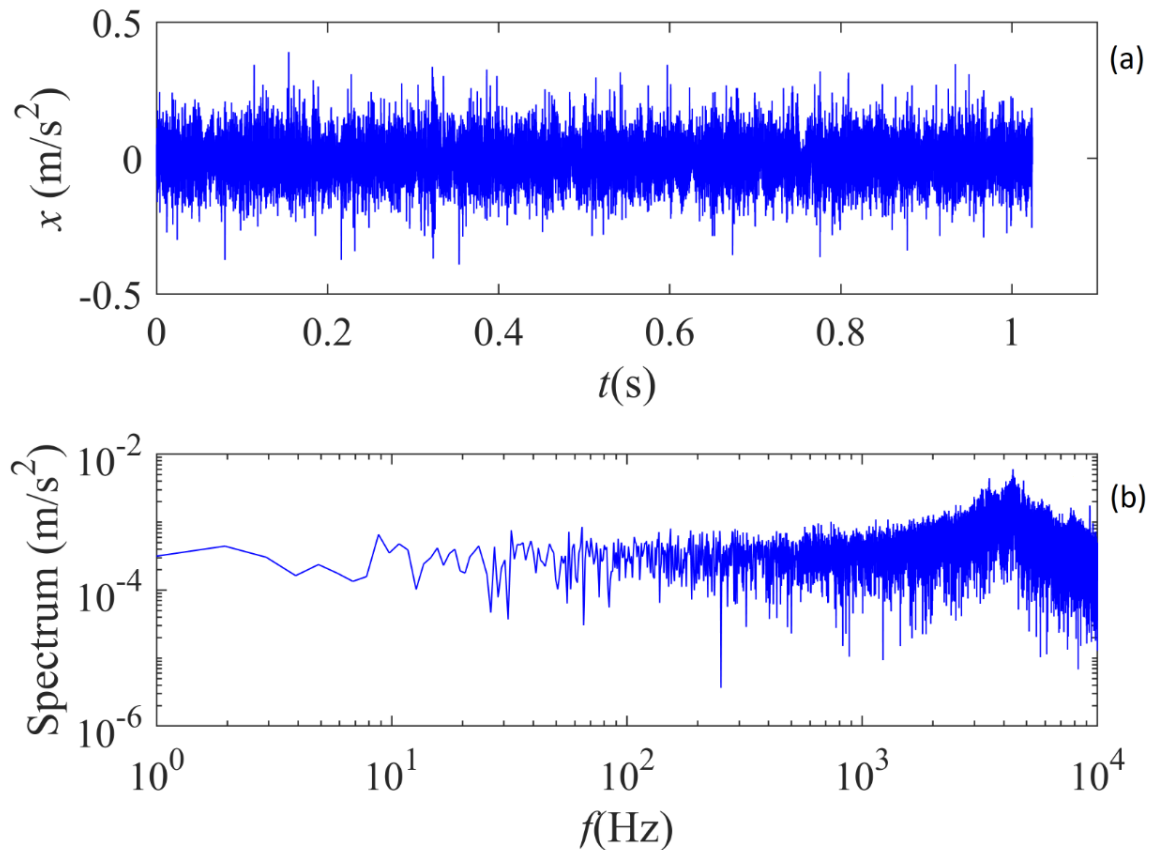


Fig.4 (a): Time domain illustration of the reference signal. (b): Frequency spectrum of the reference signal.

Datasets collected after the first 12 hours are considered as test data. For simplicity, one in every six datasets (one dataset is one hour) are chosen and their correlation coefficients with the reference signal are computed. By observing the change in correlation coefficient with respect to the increasing operation time, one can easily track down the growth of mechanical failure inside the rolling bearing over time [38]. Figure 3(b) illustrates the change in correlation coefficients as the outer race defect grows.

As can be seen from the black line in Figure 3(b), from the 12th hour to around the 85th hour, the correlation coefficients fluctuate slightly within a 0.48-0.53 range,

showing that the bearings are working in a normal state. Roughly, after the 90th hour, a clear downtrend can be observed in the plot, which indicates a gradually formed failure. The sudden drop in the correlation coefficient is caused by the high frequency resonance generated at the characteristic defect frequency. From the 90th hour to the 120th hour, as the failure develops, the difference between the reference signal and test signal becomes greater and thus leads to a higher descending rate in the plot. However, as the defect grows further, from the 120th hour to the 140th hour, the values of the correlation coefficients bounce back from 0.35 (at the 120th hour) to a peak of 0.45 (at around the 132nd hour) before experiencing another fall and finally landing at around 0.34. This sudden and drastic change may be explained by the nature of rolling bearing defect development: when the rolling element passes the defect zone, the asperities caused by the previously formed small cracks will be reduced due to over-rolling and abrasive wear. This so-called smoothing or “healing” phenomenon has been previously discovered and then verified by various researchers [39, 40]. After the 140th hour, the downward trend slows down, showing that the outer race mechanical has matured, however the continued decline of the correlation coefficients shows that bearing is still in an unstable state.

To investigate the relationship between the number of sample points and the results, plots of correlation coefficients using 10000, 8000 and 6000 sample points were drawn in Figure 3(b). From the plots, it is clear that the plot using 20480 data points fits the red fitting curve best. With fewer sample points, although the plots still follow the patterns of the fitting curve, there are larger fluctuations and the mean value decreases

and may eventually interfere with the early fault identification. As a result, through trial-and-error, we found that a minimum number of 8000 data points is needed for the method to achieve best performance.

The experiment has verified the feasibility of the proposed method. In real working conditions, due to variance in the designed tolerance for various rolling bearings, a threshold value can be set to separate normal working states from fault states. When several consecutive values are all under the threshold value, generation of mechanical failure can be identified.

3.2 Rolling Bearing Fault Classification based on Envelope signal analysis, Sample Entropy and Support Vector Machine

In section 3.1, the idea that the occurrence of a mechanical failure will cause a periodic impulse signal at a high resonance frequency is used to identify the state of the bearing. However, this feature does not help determine the type of failure or the bearing degradation state.

Fortunately, apart from the generation of impulses at resonant frequency, in the second phase of bearing failure, a series of harmonic frequency components is present at the bearing defect frequency due to the amplitude-modulation effect. According to previous studies, the defect frequency varies with the type of failure [19]. The amplitude at the defect frequency and its harmonic frequency components is small at the beginning. As the defect grows, the amplitude will become more significant. In order to use this nature of mechanical failure, EMD will first be applied to the signal to select sensitive

IMFs. There are two criteria for choosing sensitive IMFs: 1) the correlation coefficient between the IMF and the original signal must be larger than 50%; 2) The kurtosis of the IMF needs to be larger than or equal to 3. Through this process, the signal components that contain rich fault information were selected out. To further extract the features that best represent the characteristics of rolling bearing status, a feature extraction method based on envelope signal analysis is proposed.

To obtain the envelope signal, firstly, we apply a Hilbert Transform to selected IMFs:

$$H[x(t)] = \frac{1}{\pi} \sum_{-\infty}^{+\infty} \frac{c_i(\tau)}{t-\tau} d\tau \quad (13)$$

Next, the amplitude of the envelope signal can be calculated according to the equation:

$$A(t) = \sqrt{x(t)^2 + H[x(t)]^2} \quad (14)$$

To extract high quality domain features, Sample Entropy is introduced to measure the complexity of the envelope signal. Compared to directly calculating Sample Entropy from the original time domain vibration signal, applying the EMD algorithm and Hilbert transform and calculating the amplitude of envelope signal forehead decreases the effect of noise on the signal and highlights the energy concentrated at the defect frequency, which strengthens the physical justification for calculating Sample Entropy for this problem.

In this section, the first four IMFs were chosen due to their high relativity with the original signal. Thus, a $m \times 4$ feature matrix (m = number of test signals) is constructed:

$$FeatureMatrix = \begin{matrix} & IMF_1 & IMF_2 & IMF_3 & IMF_4 & \\ \begin{matrix} SaEn_1^1 \\ \vdots \\ SaEn_1^m \end{matrix} & \begin{matrix} SaEn_1^1 \\ \vdots \\ SaEn_2^m \end{matrix} & \begin{matrix} SaEn_1^1 \\ \vdots \\ SaEn_3^m \end{matrix} & \begin{matrix} SaEn_1^1 \\ \vdots \\ SaEn_4^m \end{matrix} & \begin{matrix} 1 \\ \vdots \\ m \end{matrix} \end{matrix}$$

Finally, a one-vs-one SVM model is built and optimized using the extracted features.

The original vibration data was collected at a sampling rate of 12kHz and detailed bearing dimensions are listed in Table 2.

Table 2. Detailed bearing dimensions of test rig 2

Inside diameter/mm	Outside diameter/mm	Ball Diameter/mm	Pitch Diameter/mm	Fault diameter/mm
25.0	52.0	7.94	39.04	7

There are three kinds of fault data: outer race defect, inner race defect and rolling elements defect. For every kind of mechanical fault, there are four datasets obtained under different loading conditions (Table 3). In this case, Sample Entropy parameters: $M = 2$, and $r = 0.2SD$ were chosen through a trial-and-error process.

Table 3. Illustration of all experiment datasets

Fault Type		Normal	Outer race	Inner race	Rolling elements	Load(kW)
Dataset 1	Train	80	40	40	40	0
	Test	20	10	10	10	
Dataset 2	Train	80	40	40	40	0.735
	Test	20	10	10	10	
Dataset 3	Train	80	40	40	40	1.470
	Test	20	10	10	10	
Dataset 4	Train	80	40	40	40	2.206
	Test	20	10	10	10	

As the calculation of the Sample Entropy does not rely on data length, the datasets were split into segments with 2048 data points each. Figure 5 illustrates the four bearing condition data under zero and full loading conditions using first IMFs.

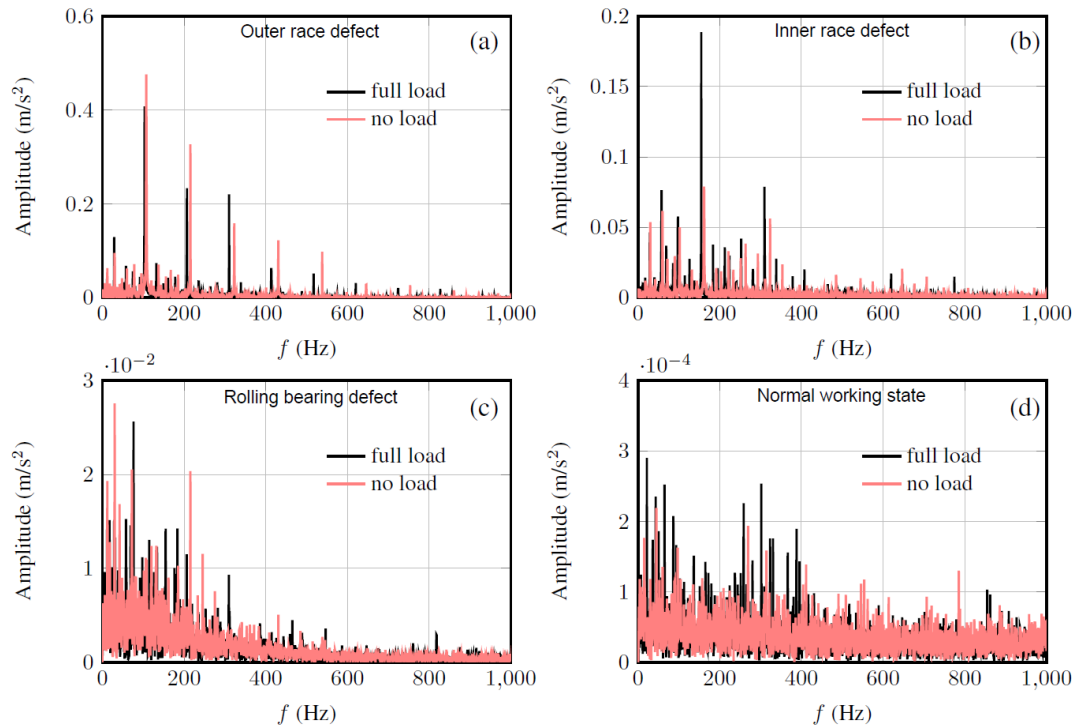


Fig.5 Envelope spectrum for four bearing status under zero and full loading conditions
 ((a) outer race defect; (b) inner race defect; (c) rolling element defect; (d) normal condition)

As can be seen from Figure 5(d), under normal conditions, the amplitudes are extremely low (10^{-4} m/s^2) and the signals are chaotic and have no periodic pattern. In all three fault conditions (Figure 5(a,b,c)), the envelope spectrums acquired under different loads share similar patterns -- there are peaks appearing at defect characteristic frequencies that correspond to one certain type of failure. Among these three fault conditions, the envelope spectrum for rolling element defects is the most chaotic: there is less difference between impulse signals at defect characteristic frequency and other components. This may be because rolling element defects, compared with other defects,

have a smaller defect surface area, thus resulting in a smaller amplitude for the impulse signal and its harmonic components. However, the peak values at Ball Spin Frequency (BSF: characteristic frequency for rolling element failure) and its harmonic components (BSF at full and no load, and $3 \times \text{BSF}$ at full load condition) are still in a dominant position. For bearing data under normal conditions (Figure 5(d)), the amplitudes are low in all frequency ranges and thus can be separated from the other three scenarios. As a result, the application of the Hilbert transform and the corresponding envelope signal can effectively extract the defect features and strengthens the physical meaning of calculating the Sample Entropy. From Figure 6, one can easily observe the great separability between Sample Entropy obtained under different fault conditions.

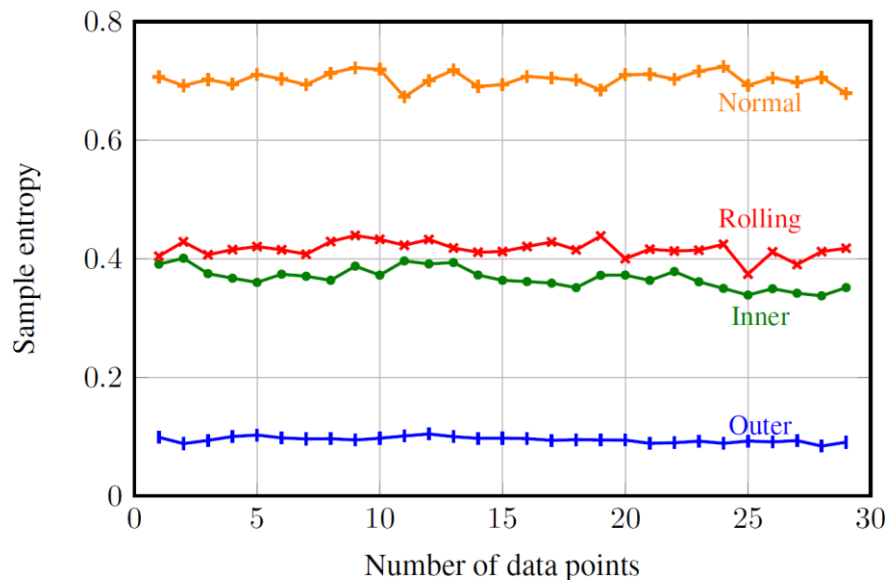


Fig. 6 Sample Entropy obtained under normal condition and three failure conditions

In this case, a six-class-one-versus-one SVM model is designed. There are 80 training samples and 20 testing samples. The overall accuracy reaches 98.5% (Figure 7). As a result, we conclude that the designed defect classification method can accurately

classify the listed kinds of mechanical failures under noisy conditions. In addition, the method works well under various loading conditions, which shows its adaptivity.

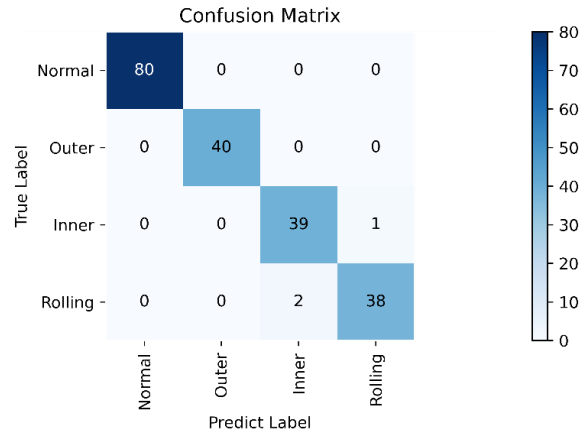


Fig.7 Confusion matrix of the proposed model

To evaluate the performance of the proposed model, deep learning models including 1D-CNN and 1D-LSTM were set up, trained and tested using the same datasets. To ensure the deep learning models achieve their best performance, data augmentation is applied to retrieve a total of 500 training samples and the same number of test samples. The results shown in Figure 8 all show very high accuracy (99.5% and 100% respectively).

Compared with SVM, deep neural networks have a relatively more complicated structure and need more datasets to train the model. In real-life, there will be cases that one cannot obtain a large number of datasets to train the model and the performance of deep learning models will be restricted. In that case, the model proposed using SVM can be utilized and achieves reliable results.

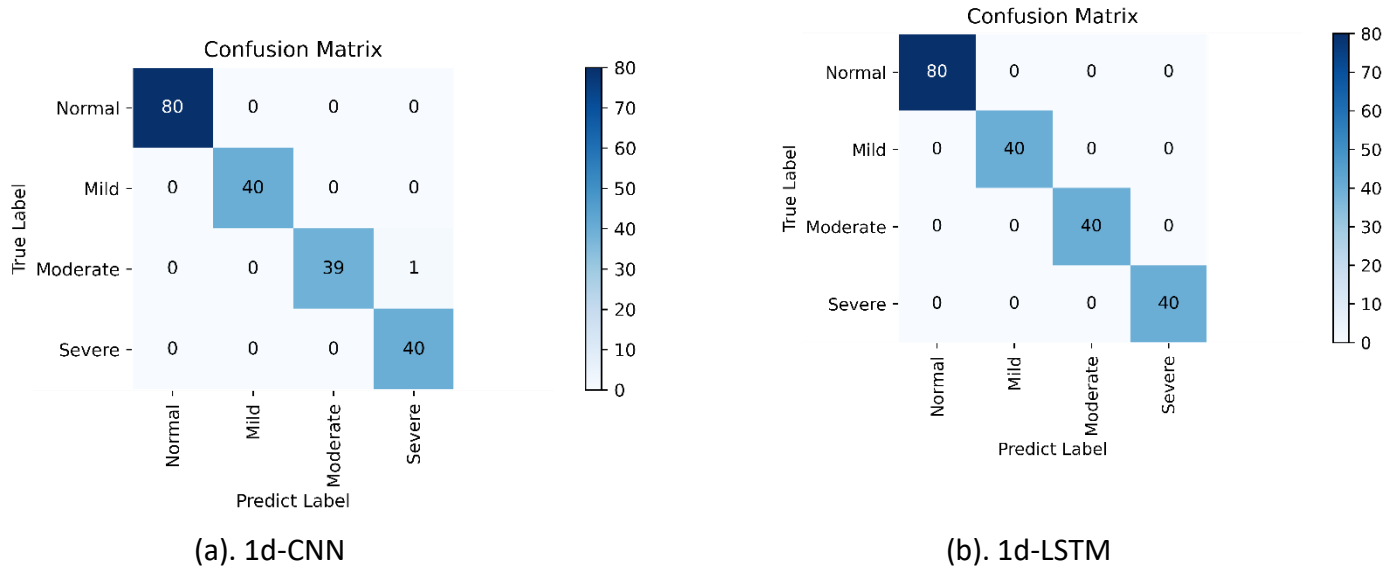


Fig. 8 Confusion matrices of the deep learning models

3.3 Bearing Degradation State Recognition

From Figure 9 (a) to (d), it is clear that with the deterioration of the failure state, a series of harmonic components appears at the defect characteristic frequency and the multiplied frequencies. Also, from Figure 9 (b) to (d), the peak amplitude at defect frequency (230Hz) keeps increasing from $2.8 \times 10^{-3} \text{m/s}^2$ to $7.2 \times 10^{-2} \text{m/s}^2$, with the later value being nearly 26 times larger than the former one. Thus, it is clear that the envelope spectrum can be used to determine the bearing degradation state.

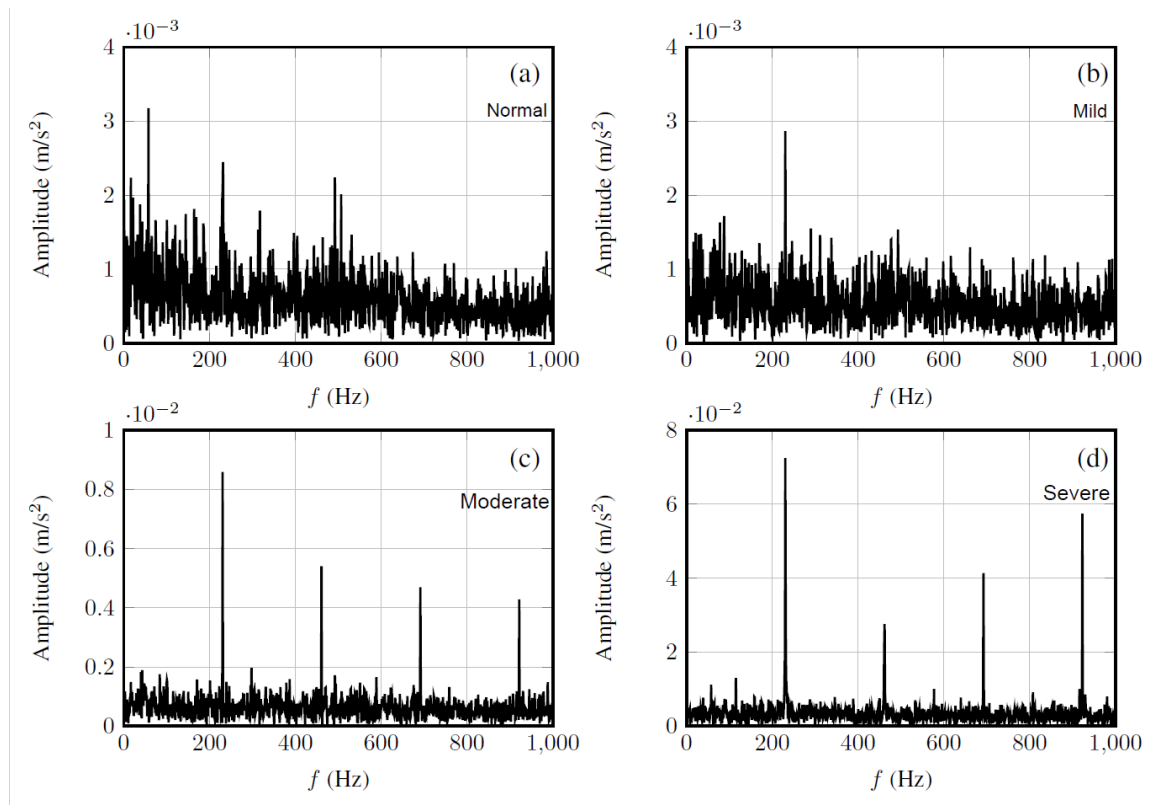


Fig.9 Envelope Spectrum under: (a) normal working state; (b) mild degradation state; (c) moderate degradation state; (d) severe degradation state

According to Figure 3 (b), the whole bearing degradation process can be roughly separated into four phases: 0-88h; 89-117h; 118-155h; 156-164h, which correspondingly separate the 984 datasets into four groups: 1-532; 533-704; 705-931; 932-984. Table 3 illustrates the degradation data partition and the composition of the training set and test set; 100 training samples and 20 test samples were chosen from each group. The training strategy used is the same as described in section 3.2.

Table 3. Degradation data partition and composition of training set and test set

Degradation states	Normal	Mild degradation	Moderate degradation	Severe degradation
Time intervals	[0,88]	[89,117]	[118,155]	[156,164]
Training samples	100 sets	100 sets	100 sets	100 sets
Test samples	20 sets	20 sets	20 sets	20 sets

Table 4. Sample entropy obtained at different degradation stages

Sample Entropy	IMF1	IMF2	IMF3	IMF4
Normal working	1.1941	0.9445	0.5261	0.2795
condition	1.1242	0.9231	0.5031	0.3019
Mild	0.9420	0.7438	0.3631	0.1827
degradation	0.9698	0.7166	0.4006	0.1611
Moderate	0.6284	0.6489	0.3598	0.1655
degradation	0.8049	0.7577	0.4108	0.1602
Severe	0.8365	0.6753	0.3949	0.1512
degradation	0.8226	0.6900	0.3749	0.1736

Table 4 contains Sample Entropy calculated for different IMFs at four degradation stages (two randomly chosen datasets for each stage). In this case, through trial-and-error, the chosen values of m and r are still 2 and 0.2SD, respectively. The value of sample entropy (SE) obtained under normal working conditions shows a clear separability from the SEs obtained from the other three degradation stages. Also, the value of SE keeps decreasing as the degradation becomes more severe: from 1.194 to 0.942 (mild degradation stage) and further descending to a value less than 0.85 (moderate and severe degradation stages). However, the dividing line between the moderate and severe

degradation states is relatively unclear: the SE obtained using IMF2,3,4 for three degradation stages shares similar values with minor fluctuations. There may be two reasons for this. Firstly, a ‘healing effect’ starts as a defect develops and weakens the defect characteristics, making them hardly detectable. The second reason is the large fluctuation over the vibration data collected among the last two stages. When using a trained SVM model to identify the degradation stages, similar results occur, as shown in Figure 10. The classification accuracy for normal working conditions and severe degradation stages are 100% and 90% respectively, while those for mild and moderate degradation stages are 65% and 50% respectively and the overall accuracy is 76.25%.

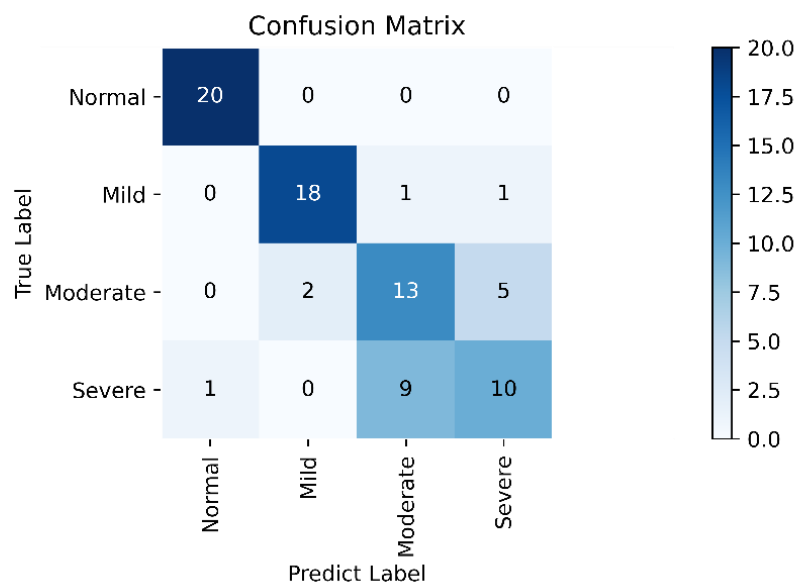


Fig.10 Confusion matrix for the bearing degradation status prediction results

To further evaluate this method, comparative experiments are also conducted in this section based on extraction of statistical time-domain and frequency-domain features . For time-domain features, a 5-dimensional feature vector is constructed:

$F_{time} = [RMS, Variance, Skewness, Kurtosis, Shape\ factor]$. For frequency-domain features, a 3-dimensional feature vector is constructed: $F_{freq} = [F_{FC}, F_{RMS}, F_{RV}]$ (centre frequency; RMS frequency and Root variance frequency). Detailed definitions and formulas for these features can be found in [4]. Thus, two feature matrices are formed and used separately to identify bearing degradation states separately through a SVM classifier:

$$FeatureMatrix = \begin{matrix} & IMF_1 & IMF_2 & IMF_3 & IMF_4 & \\ \begin{bmatrix} FV_1^1 & FV_2^1 & FV_3^1 & FV_4^1 \\ \vdots & \vdots & \vdots & \vdots \\ FV_1^m & FV_2^m & FV_3^m & FV_4^m \end{bmatrix} & & & & & \begin{bmatrix} 1 \\ \vdots \\ m \end{bmatrix} \end{matrix}$$

The classification performance of the two methods is illustrated by the confusion matrix shown in Figure 11 (overall accuracy: 51.2% and 47.5% respectively). In conclusion, although its ability to distinguish between the late and early-stage defects needs to be improved, the feature extraction method proposed in this paper can accurately indicate whether a rolling bearing system is working under normal conditions or encountering mild degradation and shows more reliable results than ordinary time-domain and frequency-domain feature extraction methods.

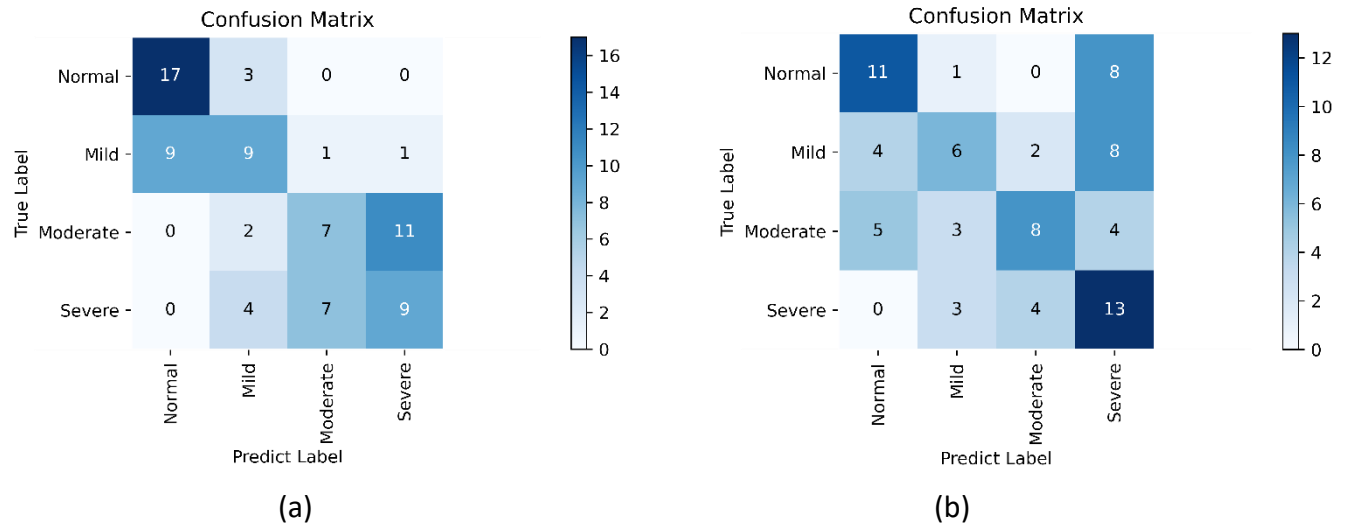


Fig. 11 Confusion matrices of bearing degradation status prediction results (a): Results using time-domain features; (b): Results using frequency-domain features

4 CONCLUSION AND FURTHER WORK

In this paper, a full diagnosis system for high-speed rolling bearings in wind turbines based on a high-quality feature extraction method and SVM is proposed. This proposed system is complete, achieving high accuracy of incipient fault diagnosis and defect classification under different loading conditions, and can automatically and efficiently extract defect features. The system also performs simple and efficient incipient fault diagnosis by computing a correlation coefficient of the test signal and comparing it with a threshold value.

In order to increase the quality of the extracted features, EMD is applied first to the raw signal to reduce ambient noise, and high frequency IMFs are chosen. Then, a Hilbert Transform is applied to demodulate the signal. The envelope signal is first obtained, followed by calculating the Sample Entropy as a feature representing the

complexity of the signal. As a result, the system is versatile and can be easily adapted to deal with various kinds of rolling bearing failure problems.

Although the system works satisfactorily when dealing with defect classification problems, the results in determining the bearing degradation stages are not always satisfactory. The separability of the Sample Entropy obtained from moderate and severe degradation stages is relatively weak and this problem is reflected by the SVM test results (65% and 50% accuracy respectively). This may be caused by the insensitive response of the Sample Entropy when dealing with signals that have energies of different intensity concentrated at similar frequencies. Thus, further studies may focus on finding a more appropriate feature that gives better results in determining the bearing degradation stages. Furthermore, real-life rolling bearing data with more complicated noise conditions may be used to test and improve the existing system.

REFERENCES

- [1] Gwec.net, 2020. [Online]. Available: <https://gwec.net/wp-content/uploads/2019/04/GWEC-Global-Wind-Report-2018.pdf>
- [2] W, Yang; P, Tavner; C, Crabtree; Y, Feng and Y, Qiu. Wind turbine condition monitoring: technical and commercial challenges. *Wind Energy*, vol. 17, no. 5, pp. 673-693, 2012.
- [3] W, Guo; Peter W, Tse; A, Djordjevich. Faulty bearing signal recovery from large noise using a hybrid method based on spectral kurtosis and ensemble empirical mode decomposition, *Measurement*, Volume 45, Issue 5, 2012.
- [4] C, Wahyu; T, Tegoeh. A Review of Feature Extraction Methods in Vibration-Based Condition Monitoring and Its Application for Degradation Trend Estimation of Low-Speed Slew Bearing. *Machines*. 5. 21. 2017.

[5] Z, He; J, Chen; T, Wang; Theories and Application of Machinery Fault Diagnosis. Higher Education Press. 06, 2010.

[6] L, Zhang; J, Xu; J, Yang; D Yang; D, Wang. Multiscale morphology analysis and its application to fault diagnosis. Mech. Syst. Signal Process. 2008, 22, 597–610.

[7] Y, Luo; C Chen; S, Kang; P, Zhang, "Fault Diagnosis of Rolling Element Bearing Using an Adaptive Multiscale Enhanced Combination Gradient Morphological Filter", Shock and Vibration , vol. 2019, Article ID 2059631, 16 pages, 2019. <https://doi.org/10.1155/2019/2059631>

[8]Lv, Chun & Zhang, Peilin & Wu, Dinghai & Li, Bing & Yunqiang, Zhang. (2020). Bearing Fault Signal Analysis Based on an Adaptive Multiscale Combined Morphological Filter. International Journal of Rotating Machinery. 2020. 1-8. 10.1155/2020/7567439.

[9] H, Lin; Y, Ye; B, Huang; J, Su. Bearing vibration detection and analysis using enhanced fast Fourier transform algorithm, Advances in Mechanical Engineering, vol. 8, no. 10, p. 168781401667508, 2016.

[10] Su, W.-S; Wang, F.-T; Zhang, Z.-X; Guo, Z.-G; Li, H.-K. Application of EMD denoising and spectral kurtosis in early fault diagnosis of rolling element bearings. 29. 18-21. 2010.

[11] B, Samanta. Gear fault diagnosis using artificial neural networks and support vector mechanics with genetic algorithms, Mech. Syst. Signal Process., 2004, 18, (3), pp. 625 – 649

[12]Saidi, Lotfi & Ben Ali, Jaouher & Bechhoefer, Eric & Benbouzid, Mohamed. (2017). Wind turbine high-speed shaft bearings health prognosis through a spectral Kurtosis-derived indices and SVR. Applied Acoustics. 120. 1-8. 10.1016/j.apacoust.2017.01.005.

[13] C.T. Yiakopoulos; I.A. Antoniadis. Wavelet based demodulation of vibration signals generated by defects in rolling element bearings, Shock and Vibration 9(2002) 293-306

[14] N.G. Nikolaou; I.A. Antoniadis. Rolling element bearing fault diagnosis using wavelet packets, NDT&E International 35(2002)197-205

[15] A, Widodo; B.S, Yang. Wavelet support vector machine for induction machine fault diagnosis based on transient current signal. Expert Syst. Appl. 2008.

[16] B, Abdel-O; C, Jean-Christophe; S, Zazia. EMD-Based Signal Noise Reduction. Signal Processing. 1. 2005.

[17] J, Guo, X, Wang, C, Zhai, J, Niu and S. Lu, "Fault diagnosis of wind turbine bearing using synchrosqueezing wavelet transform and order analysis," 2019 14th IEEE

Conference on Industrial Electronics and Applications (ICIEA), Xi'an, China, 2019, pp. 2384-2387, doi: 10.1109/ICIEA.2019.8833879.

[18] Chen, Q, Ye, M. (2014) Analysis of the Fault Diagnosis Method for Wind Turbine Generator Bearing Based on Improved Wavelet Packet-BP Neural Network. In: Li K., Xue Y., Cui S., Niu Q. (eds) Intelligent Computing in Smart Grid and Electrical Vehicles. ICSEE 2014, LSMS 2014. Communications in Computer and Information Science, vol 463. Springer, Berlin, Heidelberg. https://doi.org/10.1007/978-3-662-45286-8_2

[19] N. Huang et al., "The empirical mode decomposition and the Hilbert spectrum for nonlinear and non-stationary time series analysis", Proceedings of the Royal Society of London. Series A: Mathematical, Physical and Engineering Sciences, vol. 454, no. 1971, pp. 903-995, 1998. Available: 10.1098/rspa.1998.0193.]

[20] S. M., Pincus. "Approximate entropy as a measure of system complexity". Proceedings of the National Academy of Sciences. 88 (6): 2297–2301. 1991.

[21] J, Richman; J. Moorman. "Physiological time-series analysis using approximate entropy and sample entropy", American Journal of Physiology-Heart and Circulatory Physiology, vol. 278, no. 6, pp. H2039-H2049, 2000. Available: 10.1152/ajpheart.2000.278.6.h2039.

[22] An, X. and Pan, L. (2017) 'Wind turbine bearing fault diagnosis based on adaptive local iterative filtering and approximate entropy', Proceedings of the Institution of Mechanical Engineers, Part C: Journal of Mechanical Engineering Science, 231(17), pp. 3228–3237. doi: 10.1177/0954406216642478.

[23] Q, Ni; K, Feng; K, Wang; B, Yang; Y, Wang. A case study of sample entropy analysis to the fault detection of bearing in wind turbine, Case Studies in Engineering Failure Analysis, Volume 9, 2017, Pages 99-111, ISSN 2213-2902, <https://doi.org/10.1016/j.csefa.2017.10.002>.

[24] L, David; Mathew, Joseph. Using the correlation dimension for vibration fault diagnosis of rolling element bearings—I. Basic concepts. Mechanical Systems and Signal Processing. 1996.

[25] P.P, Kanjilal; S, Palit. On multiple pattern extraction using singular value decomposition. IEEE Trans. Signal Process. 1995, 43, 1536–1540.

[26] E, Keogh; K, Chakrabarti; M, Pazzani; S, Mehrotra. Dimensionality reduction for fast similarity search in large time series databases. Knowl. Inf. Syst. 2001, 3, 263–286.

[27] F, Cong; J, Chen; Y, Pan. Kolmogorov-Smirnov test for rolling bearing performance degradation assessment and prognosis. J. Vib. Control 2011, 17, 1337–1347.

[28] V, Sugumaran; V. Muralidharan; K I, Ramachandran. (2007). Feature selection using Decision Tree and classification through Proximal Support Vector Machine for fault diagnostics of roller bearing. *Mechanical Systems and Signal Processing*. 21. 930-942. 10.1016/j.ymsp.2006.05.004.

[29] D. Pandya, S. Upadhyay and S. Harsha, "Fault diagnosis of rolling element bearing by using multinomial logistic regression and wavelet packet transform", *Soft Computing*, vol. 18, no. 2, pp. 255-266, 2013. Available: 10.1007/s00500-013-1055-1.

[30] Lin, C.-J. et al. (2019) 'Diagnosis of ball-bearing faults using support vector machine based on the artificial fish-swarm algorithm', *Journal of Low Frequency Noise, Vibration and Active Control*. doi: 10.1177/1461348419861822.

[31] W, Zhang; G, Peng; C. Li; Y, Chen; Z, Zhang; X, Wang. A New Deep Learning Model for Fault Diagnosis with Good Anti-Noise and Domain Adaptation Ability on Raw Vibration Signals. *Sensors* 2017, 17, 425.

[32] Han Liu, Jianzhong Zhou, Yang Zheng, Wei Jiang, Yuncheng Zhang, Fault diagnosis of rolling bearings with recurrent neural network-based autoencoders, *ISA Transactions*, Volume 77, 2018, Pages 167-178, ISSN 0019-0578, <https://doi.org/10.1016/j.isatra.2018.04.005>.

[33] Z, Zhuang; H, Lv; J, Xu; Z. Huang; W, Qin. "A Deep Learning Method for Bearing Fault Diagnosis through Stacked Residual Dilated Convolutions", *Applied Sciences*, vol. 9, no. 9, p. 1823, 2019. Available: 10.3390/app9091823.

[34] V, Vapnik. *The nature of statistical learning theory*. New York: Springer, 2010.

[35] G, Hu. *Introduction to Digital Signal Processing*, 2nd ed. Beijing: Tsinghua University Press, 2013, pp. 22-24.

[36] J, Lee; H, Qiu; G, Yu; J, Lin; and Rexnord. Technical Services (2007). IMS, University of Cincinnati. "Bearing Data Set", NASA Ames Prognostics Data Repository (<http://ti.arc.nasa.gov/project/prognostic-data-repository>), NASA Ames Research Center, Moffett Field, CA

[37] Loparo, K. *Bearings Vibration Data Set*, Case Western Reserve University. Available online: http://www.eecs.case.edu/laboratory/bearing/welcome_overview.htm.

[38] Pankaj Gupta, M.K Pradhan, Fault detection analysis in rolling element bearing: A review, *Materials Today: Proceedings*, Volume 4, Issue 2, Part A, 2017, Pages 2085-2094, ISSN 2214-7853, <https://doi.org/10.1016/j.matpr.2017.02.054>.

[39] H, Li et al. "A Novel Health Indicator Based on Cointegration for Rolling Bearings' Run-To-Failure Process." *Sensors* (Basel, Switzerland) vol. 19,9 2151. 9 May. 2019

[40] T, Williams. "Rolling Element Bearing Diagnostics in Run-to-FAILURE Lifetime Testing", *Mechanical Systems and Signal Processing*, vol. 15, no. 5, pp. 979-993, 2001. Available: 10.1006/mssp.2001.1418.